Journal of Food Protection, Vol. 60, No. 3, 1997, Pages 309–314

Acoustic Imaging of Defects in Flexible Food Packages

AMJAD A. SAFVI,[1] HAROLD J. MEERBAUM,[2] SCOTT A. MORRIS,[2]
CAROL L. HARPER,[3] and WILLIAM D. O'BRIEN, JR.[1]*

[1]*Bioacoustics Research Laboratory, Department of Electrical and Computer Engineering,* [2]*Departments of Food Science & Human Nutrition and Agricultural Engineering, and* [3]*Department of Food Science & Human Nutrition, University of Illinois, Urbana, Illinois 61801, USA*

(MS# 96-101: Received 22 April 1996/Accepted 30 July 1996)

ABSTRACT

A study was conducted using a high-frequency acoustic imaging system, the scanning laser acoustic microscope (SLAM), operating at 100 MHz, to detect packaging defects to within the system's resolution limit of 20 μm. The purpose of the study was to assess the feasibility of high-frequency acoustic imaging to detect and classify channel defects that would have the potential for microbial contamination through visually undetected defects. The SLAM can characterize and image various materials and defects by exploiting the differences in acoustic (mechanical) transmission properties within different materials. Channel defects transverse to the heat-seal major axis were fabricated by sandwiching 10-, 16-, 25-, and 37-μm wire between two layers of either polyethylene or plastic retort-pouch laminate film which were then heat sealed. The wire was then pulled out, leaving a channel filled variously with saline solution, air, or both. The channel defects were then assessed using the SLAM and validated with confocal microscopy. The results indicate that the SLAM technology can readily detect channel defects as small as 10 μm, the smallest channel defects examined, which is one-half the imaging system stated resolution specification. This study has clearly demonstrated that acoustic microscopy can nondestructively image micrometer-scale channel defects in heat seals at and smaller than the SLAM's resolution limit.

Key words: Acoustic imaging, food, packaging, defects, scanning laser acoustic microscope

---

The physical dimensions and mobility of most types of pathogenic organisms are well documented. Similarly, studies have been done to determine the ability of microorganisms to penetrate membranes with intentionally included micrometer-size defects. What is not yet known is the lower limit of the ability of pathogenic microorganisms to penetrate a transverse channel formed in a heat-sealed package. Table 1 presents a compilation of defect sizes that have resulted from the work of various researchers. The defect sizes range widely as did the experimental conditions, giving no clear-cut lower limit. Preliminary estimates of a 10-μm lower size limit have been proven false, pointing out the need for a better understanding of the size limits for seal defects in packages of this type.

Heat seals in packages are usually formed by applying thermal energy to the contacting surface of the layers of materials to be sealed, either directly by heat conduction or indirectly by high-frequency electromagnetic induction. All of these types of seals are subject to the formation of defects from a variety of sources. Wrinkles in the materials, inclusion of foreign materials—including the packaged food itself—and post sealing mechanical damage are all sources of defects which may compromise the microbial barrier of the package.

Current methods of quality control depend on (human) visual inspection for defects (as mandated by the U.S. Code of Federal Regulations in 9CFR381.301(d) and by 21CFR113) and hold-and-inspect methods by process batch where entire production lots are held and inspected for evidence of microbial growth after a suitable incubation period. With global canned-food production in the tens of billions of cans per year, neither of these inspection methods are fast enough to allow the economical substitution of newer types of heat-sealed packages for metal cans and jars when packaging low-acid and other types of especially pathogen-susceptible foodstuffs.

From a previous broad-scale survey *(10)* and trials of leak-detection methods, acoustic imaging was left, by elimination, as the best alternative for the development of a sensor which would provide the needed sensitivity, spatial resolution, and temporal resolution (when used as a dedicated linear scanning sensor to provide high feed-through speeds). Acoustic imaging in the frequency range which yields micrometer-scale spatial resolution is termed acoustic microscopy. Because the acoustic microscope uses the change in mechanical properties from point to point to achieve image contrast, and because ultrasound can penetrate opaque materials to a limited depth, the information obtained by the acoustic microscope can offer new insights into the micromechanical behavior of thin materials and thin bonded materials.

A scanning laser acoustic microscope (SLAM) was used in this study. It is a transmission microscope that can image bulk properties of a thin specimen and can determine point-by-point measurements of the bulk wave ultrasonic-propagation properties. This class of transmission acoustic microscopes operates in the frequency range between 10 and 500 MHz and has corresponding spatial resolution in the

* Author for correspondence. Tel: 217-333-2407; Fax: 217-244-0105; E-mail: wdo@uiuc.edu

range between 200 and 4 μm, respectively. Generally, transmission acoustic microscopes are sensitive to bulk transmission-property variations. SLAM uses transmitted sound waves instead of light to produce images, and has the documented ability to detect, classify, and accurately reproduce the internal structure of opaque materials and the defects contained therein. Acoustic-imaging techniques (virtually all of which use pulse-echo techniques at lower frequencies and, thus, lower resolution) have successfully been used to detect voids, flaws, and cracks in epoxy-fiber composites, metals, and biological materials *(3)*.

The long-term goal of this research is the development of an on-line, real-time, nondestructive package integrity evaluation system. The short-term goal is to further the state of the art of detecting and classifying channel defects that will compromise the integrity of new types of food packages by using a research-team (experts in packaging, acoustic imaging, and challenge testing) approach. One of the specific aims of this research is to establish the factors affecting the performance of acoustic imaging in the types of polymeric materials which are typically used in food-packaging applications. Specifically these include factors such as imaging conditions, thickness and composition of materials, and void geometry.

The hypothesis to be tested in this study was whether or not the scanning laser acoustic microscope is capable of accurately detecting and characterizing artificially created voids in heat-sealed packaging materials. The results will indicate whether or not acoustic imaging, as the leading candidate for nondestructive package-testing methodology, has potential for the development of on-line testing methods.

MATERIALS AND METHODS

Channel defect manufacture

Channel defects were prepared by placing different size tungsten wires (10, 16, 25, and 37 μm in diameter) (California Fine Wire Company, Grover City, CA) between two layers of plastic material, either polyethylene film taken from commercially available food bags (Ziploc® brand, DowBrands L.P., Indianapolis, IN) or plastic microwavable retort-pouch material (Fuji Tokushu Shigyo Co., Ltd., Seto Aichi, Japan). The thickness of one layer of the polyethylene film was 68 μm and that of the plastic laminate film was 115 μm. The tungsten wire was sealed into place using an automatic heat sealer (Doboy HS-C2420 51, Doboy Co., New Richmond, Wisconsin) at a sealing temperature of 109°C for the polyethylene film and 132°C for the plastic-laminate microwavable-pouch film. The wire was then pulled out leaving cylindrically shaped channels. A small region of the channel defect was cut out by using a razor blade and placed on the acoustic microscope stage for imaging, taking care not to disturb the channel region to be imaged. Some samples were also frozen and cut to preserve geometry of the channel (for independent characterization of the channel with a confocal microscope) using a cryomicrotome (Lipshaw Electric Cryo Microtome, Model 1500, Detroit, MI).

TABLE 1. *Minimum defect size for bacterial penetration*

Defect size[a] (μm)	Test characteristics	Reference
0.2	filtration of certain waterborne bacteria	*(11)*
11	immersion test on pouches	*(13)*
22	immersion test on pouches	*(7)*
80	electrolytic test on aseptic packages	*(1)*
10	immersion test on vials	*(4)*
5	spray on vials	
10	predictive equation	*(6)*
≈10	aerosol test	*(12)*
<10	immersion test	
<10	biocell test	*(9)*
<7	microperfusion test	*(15)*

[a] Defect sizes based on *(6)* and updated by *(2)*.

Scanning laser acoustic microscope measurements

A scanning laser acoustic microscope (Sonomicroscope 100®, Sonoscan, Inc., Bensenville, IL 60106), operating at an acoustic frequency of 100 MHz, was used to examine the channels in a double-layer 230 μm plastic-laminate microwavable retort pouch and in a double-layer 136 μm polyethylene film, as well as to estimate the speed of sound and the attenuation coefficient. Operational details of the scanning laser acoustic microscope (SLAM) have been published previously *(5, 14, 16, 17, 18)*. Briefly, the specimen is placed on a sonically activated fused-silica stage along with a thin layer of normal saline and covered with a semireflective coverslip. A focused scanning laser-beam probe detects a dynamic ripple (surface displacement) by reflection from the coverslip lower surface. The reflected laser beam is processed to yield the acoustic image, from which the attenuation coefficient is determined, and the interference image, from which the propagation speed is determined. The laser beam also is transmitted through the specimen to yield an optical image. All three images are displayed in real time on standard television monitors. The image's field of view is approximately 3 mm horizontally by 2 mm vertically (typically 100×). A frame grabber was used to digitize the video signal of the acoustic and interference images and performed frame averaging (up to 256 frames), convolutions (for filtering), and histograms (for dynamic range determination). Propagation speed (from the interference image) and attenuation coefficient (from the acoustic image) estimates were performed in software utilizing the digitized video image; quantitative assessment of propagation speed and/or attenuation coefficient provides the basis for understanding the mechanisms responsible for image contrast, for estimating spatial resolution, and for estimating imaging depth of penetration. The SLAM images were saved as a binary image file, converted back to a TIFF (tagged-image file format), and processed in Adobe Photoshop 3.0 (Mountain View, CA, USA).

Propagation speed. The spatial frequency domain technique is used to yield longitudinal propagation speed from the interference image *(16, 18)*. The interference image field of view contains approximately 39 vertical interference lines equally spaced by about 85 μm for the 100-MHz SLAM. The unknown propagation speed, c_x, is estimated by the horizontal shift, N, of the fringe lines relative to where the fringe lines would be without the specimen, that is, relative to the reference (known) speed, c_o, by the expression *(8)*

$$c_x = \left(\frac{c_o}{\sin\theta_o}\right) \sin\left(\tan^{-1}\left(\frac{1}{\frac{1}{\tan\theta_o} - \frac{N\lambda_o}{T\sin\theta_o}}\right)\right), \quad (1)$$

where θ_o is the sound propagation direction in the reference medium relative to the normal, λ_o is the wavelength of sound in the reference medium and T is the specimen thickness. The specimen is positioned with the channel defect in the center of the interference

image (Fig. 1a). From the digitized interference image, each interference line region (a horizontal width of 32 μm) is digitized and processed to yield a vertical speed profile (Fig. 1b).

Attenuation coefficient. An insertion loss procedure is used to estimate the attenuation coefficient *(16, 17).* In principle, this procedure compares the received signal amplitude of the specimen of known thickness in the sound path with that of the reference medium, normal saline solution. A subimage area for the 100-MHz SLAM is approximately 400 by 250 μm (96 pixels horizontally by 32 pixels vertically) in the acoustic image. The signals received from the subimage area are then digitized to yield an average amplitude value (V). A minimum of five V values are recorded for the reference (known) medium. The specimen then is moved into the subimage area and a minimum of five values of V are recorded at each of five separate specimen locations within each of the two specimen regions. An insertion loss (IL) value, in dB, is estimated from

$$IL = V_s - \langle V_r \rangle, \tag{2}$$

where $\langle V_r \rangle$ is the mean value of V recorded from the reference (known) medium, and V_s are the individual values of V from the specimen. This process yields a minimum of five IL values for each specimen thickness from adjacent spatial regions.

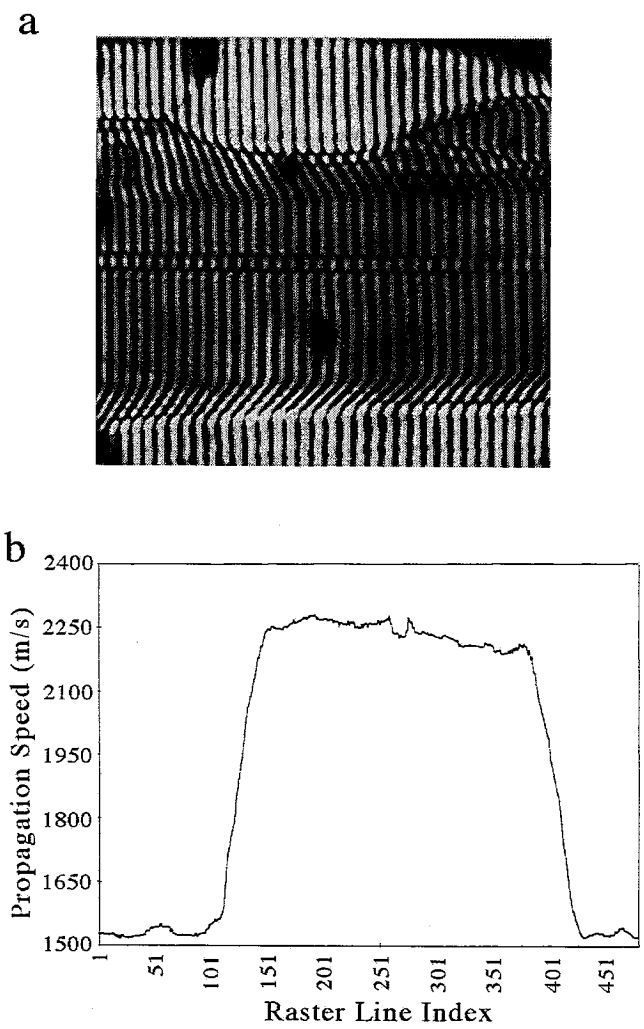

FIGURE 1. *(a) Acoustic-interference image of a 15-μm channel defect in polyethylene film and (b) a propagation-speed profile taken from the middle of the interference image. The left side of the speed profile represents the top of the interference image and the right side represents the bottom.*

Confocal microscope measurements

Validation of the sample in terms of channel size and distinctive features was achieved using a Zeiss confocal laser scanning microscope. The confocal microscope can produce topographical images and can make measurements on the image with a resolution of 0.5 μm. The microscope was used to measure channel diameter with an end view and a side view. The side view also showed the uniformity of the channel diameter. He-Ne 543-nm and Ar 514-nm lasers were used as the light source. In confocal mode, the depth of field is in the range of a few micrometers so that a topographical image can be obtained. Various filters, diaphragm, and condenser settings were used to optimize the image prior to image processing.

Image processing

Gray-scale images were obtained from the SLAM and the confocal microscope in a digitized form. The images were transferred to a Quadra 950 Macintosh computer. Using the program Adobe Photoshop 3.0 (Adobe Systems Inc., Mountain View, CA), image intensity was adjusted to bring out salient features, and the images were arranged by channel size and type of material used (polyethylene or plastic laminate). Various image-enhancing filters and brightness/contrast controls were used to optimize the gray-scale images. Images were despeckled using a noise filter and final images were printed with a Phaser IIsdx color printer (Tektronix Inc., Beaverton, OR).

RESULTS

Scanning laser acoustic microscope optical and interference images

The SLAM optical and interference images were generated from the plastic laminate and polyethylene film channels which were fabricated from the four different wire diameters (10, 16, 25, and 37 μm). SLAM optical and interference images of a 10-μm channel (opaque versus nonopaque) in plastic laminate and polyethylene are shown in Figures 2 and 3, respectively. The channels in these figures were filled with saline solution as determined from the real-time SLAM optical image by observing the saline capillating through the channel; additionally, a left shift of the interference lines from the SLAM interference image was observed in the channel, a left shift which resulted because the saline propagation speed is lower that that of the plastic.

The fact that ultrasound can pass through various opaque materials is useful in imaging food packages that are colored or overprinted. Figures 2 and 3 show two cases of 10-μm channel defects in plastic laminate and polyethylene, one which is optically transparent (left side) and the other which is partially opaque (right side). The interference images in both figures, shown with and without opacity, clearly image the channel.

Confocal microscopy

Based on confocal microscope measurements, the four different channel diameters in plastic laminate corresponded well to the respective wire diameters used to create the

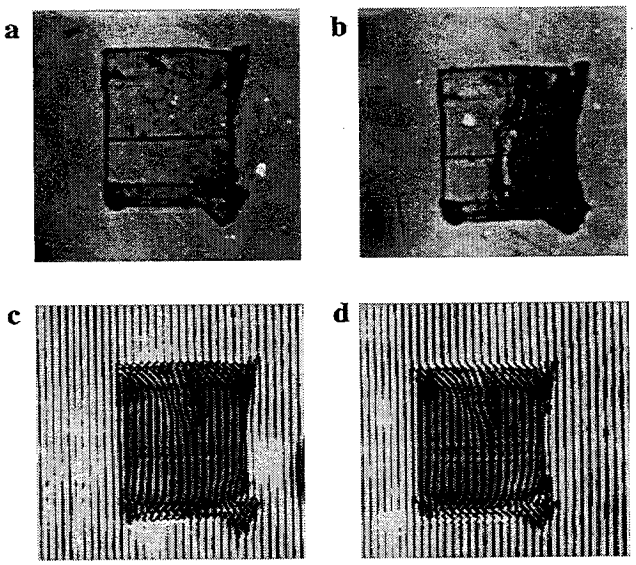

FIGURE 2. *SLAM optical (a and b) and interference (c and d) images of a 10-μm channel defect in plastic laminate film. The left two images (a and c) are optically transparent whereas the right two images (b and d) have had the right side of the sample made optically opaque.*

channel (Fig. 4). All of the defects corresponded well with a circular-shaped channel when imaged end-on with the confocal microscope. Results for the plastic laminate samples having diameters of 10, 16, 25, and 37 μm were shown to be repeatable by fabricating a new set of laminate samples three times and measuring their diameters by means of confocal microscopy. There was a 3 to 5% difference between the channel diameters measured by the confocal microscope and that of the actual wire diameters (Table 2). This 3 to 5% error is within the resolution limits of the confocal microscope.

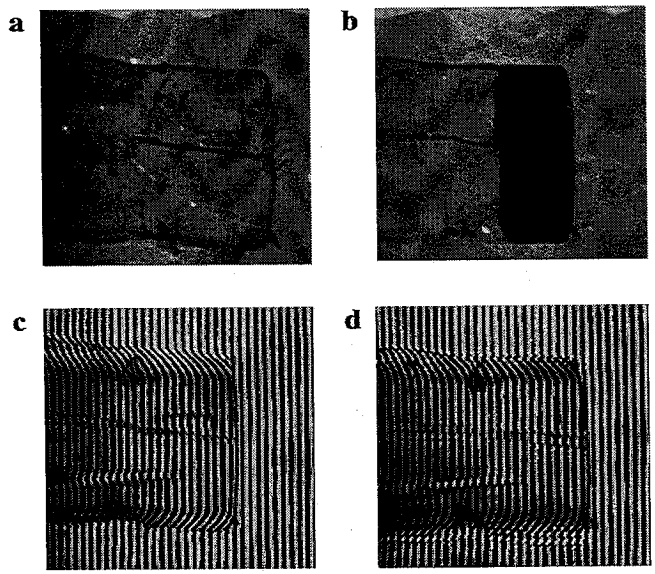

FIGURE 3. *SLAM optical (a and b) and interference (c and d) images of a 10-μm channel defect in polyethylene film. The left two images (a and c) are optically transparent whereas the right two images (b and d) have had the right side of the sample made optically opaque.*

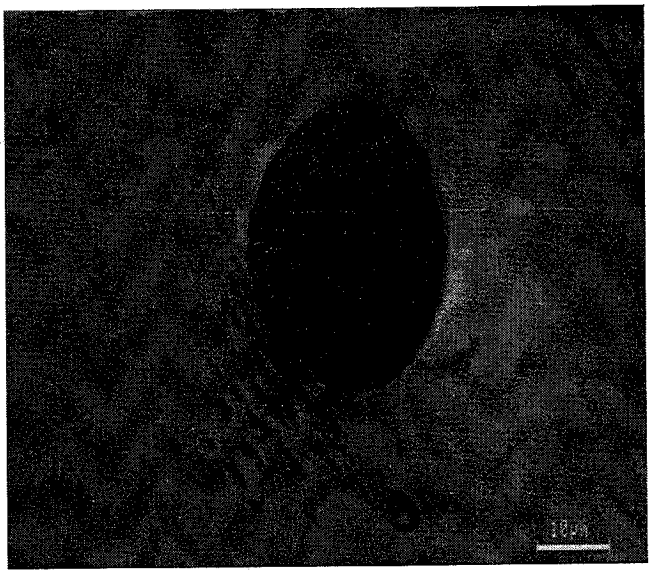

FIGURE 4. *Example of a confocal microscope image of a 25-μm channel defect in plastic laminate film (end view).*

Scanning laser acoustic microscope measurements

Propagation speed. Propagation speed was determined for 9 samples each for both plastic laminate and polyethylene films. A speed profile was generated for each individual sample of known thickness. The propagation speed was averaged at various locations of the plastic film, and then those values were averaged. The single-layer polyethylene samples had a thickness of 68 μm and the single-layer plastic laminate samples had a thickness of 115 μm. Saline solution was used for the reference speed (1520 m/s). For plastic laminate film the propagation speed (mean and standard deviation) was 2376 ± 24 m/s and that for the polyethylene film was 2322 ± 25 m/s. A reduction in speed of approximately 4% was detected at the channels of both sample films relative to the propagation speeds of the films.

Attenuation coefficient. The attenuation coefficient was determined for 5 samples each of both plastic-laminate and polyethylene films. The *IL* was determined for three thicknesses (1, 2 and 3 layers) of each plastic film (68, 136 and 204 μm for polyethylene; 115, 230 and 345 μm for plastic laminate). The attenuation coefficient was then determined from the *IL* versus thickness slope by performing a linear regression. For plastic-laminate film the attenuation coefficient (mean and standard deviation) was 58 ± 8 dB/mm and

TABLE 2. *Comparison of the diameter of wire used to create channel defects and channel diameters in plastic trilaminate measured on confocal images*

Wire diameter (μm)	Channel diameter, mean ± SD, $n = 10$ (μm)
10	10.7 ± 0.78
16	15.3 ± 1.17
25	24.9 ± 0.68
37	38.5 ± 1.45

that for polyethylene film was 90 ± 6 dB/mm, all values at an ultrasonic frequency of 100 MHz.

DISCUSSION

Channel defects in polyethylene film were more readily detectable than in plastic-laminate film due to the lesser thickness of the polyethylene plastic (136 μm for two-layer polyethylene versus 230 μm for two-layer laminate) which affected total sound transmission through the samples (insertion loss through polyethylene of 12 dB versus 13 dB through laminate). This was compensated to a certain extent by using image processing (brightness/contrast filters) to bring out salient features. The channel size assessed from the acoustic images of the smaller channel diameters (10 to 25 μm) did not correspond well to the diameters of the channel defects. A possible explanation for the inability to estimate channel diameters near the resolution limit of the SLAM is attributed to the diffraction-limited capability of imaging techniques in general, so that the SLAM can be used to identify (detect) the existence of a defect channel, but defect diameter differences cannot be easily resolved when operating close to the SLAM resolution limit of 20 μm. For larger defect diameters (37 μm), the channel size is more clearly and accurately defined in the acoustic image, as expected.

In the saline-solution-filled channels, a reduction in propagation speed (indicated by a left shift of the vertical interference lines in the channel area) occurred in the interference image for both polyethylene and plastic laminate channels. The propagation speed of saline is approximately 1520 m/s, which is less than the values obtained for the plastics (2376 ± 24 m/s for plastic laminate and 2322 ± 25 m/s for polyethylene). The propagation-speed difference between saline and the plastic film specimens is much greater than that observed experimentally (about 4%) and is attributed to the fact that the channel diameters investigated were less than an acoustic wavelength, thus suggesting that the measured propagation speed included the plastic film both in and near the channel defect. In other words, the resolution capability was such that it was not possible to quantitate the propagation speed solely in the channel.

This study has clearly demonstrated that acoustic microscopy can nondestructively image micrometer-scale channel defects in heat seals irrespective of the optical properties of the material as well as any sort of inclusions in the seal area. The implications are that an acoustical method may prove to be the basis for the development of an accurate on-line sensor capable of 100% inspection of heat seals at production-line speeds. Such a sensor should eliminate the economic bottleneck which has restrained the widespread use of these types of packages. The improvement in product quality associated with these types of packages coupled with assured safety and lowered production costs will result in a safer, cheaper, higher-quality food supply for the consumer.

The results obtained significantly exceeded the expected results. A 10-μm channel defect was *detected* using a SLAM with a 20-μm resolution limit. However, a 10-μm channel defect could not be *characterized* in terms of an accurate dimensional measurement. If it were necessary to characterize channel defects in the 10-μm diameter range, higher-frequency acoustic microscope technology could be used. The spatial resolution limit of the SLAM is inversely proportional to frequency. Therefore, when the frequency is doubled, the resolution limit is halved. On the basis of our results, if a 500-MHz SLAM were used (resolution limit about five times smaller than the 100 MHz SLAM, that is, 4 μm), channel defects smaller than 10 μm should not only be detectable but also able to be characterized. However, as ultrasound frequency is increased, penetration depth decreases, because the attenuation coefficient is frequency dependent. This trade-off between imaging depth and resolution may limit the depth of defect detection in food packaging.

This study has demonstrated the use of high-frequency ultrasound to be an effective and precise way to image channel defects in certain food-packaging materials. This work can lead to further classification of various food-packaging defects and eventually to the development of an on-line imaging and evaluation system.

ACKNOWLEDGMENT

The authors would like to acknowledge the financial support from the Value-Added Research Opportunities Program, Agricultural Experiment Station, University of Illinois.

REFERENCES

1. Axelson, L., S. Clavin, and J. Nordstrom. 1990. Aseptic integrity and microhole determination of packages by electrolytic conductance measurements. Pack. Technol. Sci. 3:141–162.
2. Blakistone, B. 1994. New developments in plastic packaging seal integrity testing: one key to the future of high speed plastic packaging, p. 1–18. Proceedings of IoPP Packaging Technology Conference: New and Emerging Developments in Packaging Technology. Institute of Packaging Professionals, Herndon, VA.
3. Briggs, A. 1992. Acoustic microscopy. Clarendon Press, Oxford.
4. Chen, C., B. Harte, C. Lai, J. Pestka, and D. Henyon. 1991. Assessment of package integrity using a spray cabinet technique. J. Food Prot. 54:643–648.
5. Embree, P. M., K. M. U. Tervola, S. G. Foster, and W. D. O'Brien, Jr. 1985. Spatial distribution of the speed of sound in biological materials with the scanning laser acoustic microscope. IEEE Trans. Sonics Ultrason. SU-32:341–350.
6. Floros, J. D., and V. Gnanasekharan. 1992. Critical leak size and package integrity, p. 157–188. *In* Advances in aseptic processing technology. Elsevier, New York.
7. Gilchrist, J. E., D. B. Shah, D. C. Radle, and R. W. Dickerson, Jr. 1989. Leak detection in flexible retort pouches. J. Food Prot. 52:412–415.
8. Goss, S. A., and W. D. O'Brien, Jr. 1979. Direct ultrasonic velocity measurements of mammalian collagen threads. J. Acoust. Soc. Am. 65:507–511. Erratum: J. Acoust. Soc. Amer. 65:1582.
9. Harper, C. L. 1994. Unpublished data.
10. Harper, C. L., B. A. Blaikstone, J. B. Litchfield, and S. A. Morris. 1995. Developments in food package integrity testing. Trends Food Sci. Technol. 6:336–340.
11. Howard, G., and R. Duberstein. 1908. A case of penetration of 0.2 micron rated membrane filters by bacteria. J. Parenteral Drug Assoc. 34:95–102.
12. Keller, S., J. March, and B. Blakistone. 1994. Unpublished data.
13. Lampi, R. A. 1980. Retort pouch: the development of a basic packaging concept in today's high technology era. J. Food Process Eng. 4:1–18.
14. Nicozisin, D. D. 1989. An automated image data acquisition and analysis system for the scanning laser acoustic microscope. Master of

Science Thesis, Department of Electrical and Computer Engineering, University of Illinois, Urbana, IL.

15. Rose, D. 1994. Risk factors associated with post process contamination of heat sealed semi-rigid packaging. Technical Memorandum no. 708. Campden & Chorleywood Food Research Association, Chipping Campden, U.K.
16. Steiger, D. L., W. D. O'Brien, Jr., J. E. Olerud, M. A. Riederer-Herderson, and G. F. Odland. 1988. Measurement uncertainty assessment of the scanning laser acoustic microscope and application to canine skin and wound. IEEE Trans. Ultrason. Ferroelec. Freq. Contr. 35:741–748.
17. Tervola, K. M. U., S. G. Foster, and W. D. O'Brien, Jr. 1985. Attenuation coefficient measurement technique at 100 MHz with the scanning laser acoustic microscope. IEEE Trans. Sonics Ultrason. SU-32:259–265.
18. Tervola, K. M. U., and W. D. O'Brien, Jr. 1985. Spatial frequency domain technique: an approach to analyze the scanning laser acoustic microscope. IEEE Trans. Sonics Ultrason. SU-32:544–554.